RSC Advances

ROYAL SOCIETY OF CHEMISTRY

www.rsc.org/advances

Journal Name

RSCPublishing

ARTICLE

Synchronously synthesized Si@C composites through solvothermal oxidation of Mg_2Si as lithium ion battery anode

Cite this: DOI: 10.1039/x0xx00000x

Received ooth January 2012,
Accepted ooth January 2012

DOI: 10.1039/x0xx00000x

www.rsc.org/

Zhiguo Hou,[a] Xueqian Zhang,[a] Jianwen Liang,[a] Xiaona Lia,[a] Xuedong Yan,[b] Yongchun Zhu[a,*] and Yitai Qian,[a,*]

Si@C composites have been solvothermally synthesized by the reaction of ethanol or acetone with Mg_2Si at 650 ^oC, followed by HCl washing. Ethanol or acetone can oxidate Mg_2Si to form Si, and at the same time, they are reduced to synchronously form carbon coated on the surface of the generated Si nanoparticles. As lithium ion battery anode, the as-synthesized Si@C composites obtained from the reaction of acetone with Mg_2Si deliver a reversible capacity of 3277 mA h g^{-1} at 0.36 A g^{-1} and remain 892 mA h g^{-1} at 3.6 A g^{-1} after 350 cycles.

1. Introduction

Silicon has been one of the most studied anode materials for lithium ion batteries because of its abundance in nature, high theoretical capacity (3600 mA h g^{-1}) and relatively low working potential (< 0.5 V *versus* Li/Li^+).[1-5] However, the serious volume change (over 300%) during lithium insertion/extraction results in the rapid capacity loss.[6, 7] Using nanostructured Si and carbon coating are two effective strategies to face these problems.[8-11]

Numerous methods have been employed to prepare Si nanomaterials with carbon coating, which dramatically improved the lithium storage properties of Si anode. Cui et al. prepared Si nanowires and nanoparticles encapsulated in carbon hollow tubes or amorphous carbon layer, in which dispersed Si nanoparticles were coated by carbon layer through annealing polymer coating.[12-15] Yolk-shell structure Si@C composites prepared by this two step method exhibited a high capacity of 2800 mA h g^{-1} at 0.36 A g^{-1}, and 1300 mA h g^{-1} capacity remained after 1000 cycles at 3.6 A g^{-1}.[13] Hollow core–shell structured porous Si@C nanocomposites were prepared through employing acetylene to coated carbon layer on calcined Si nanoparticles. The as-synthesized Si@C composites showed 920 mA h g^{-1} at 0.1 A g^{-1}, and remained 460 mA h g^{-1} after 300 cycles at 1 A g^{-1}.[16] Recently, core–shell Si/C nanospheres embedded in bubble sheet-like carbon film were synthesized through magnesium reduction SiO_2 to hollow Si nanospheres, at the same time, the glucose converted to carbon layer on Si surface.[17] The as-prepared Si/C composite exhibited 1286 mA h g^{-1} at 0.5 A g^{-1} and remained 1018 mA h g^{-1} after 200 cycles at 1 A g^{-1}.

Conversion of Mg_2Si into Si is a favourable route to obtain nanostructure Si anode materials. Si nanoparticle anodes obtained by the reaction of Mg_2Si with $ZnCl_2$ showed a reversible capacity of 795 mA h g^{-1} at 3.6 A g^{-1} over 250 cycles.[18] Nanoporous silicon anodes synthesized through the reaction of Mg_2Si and molten bismuth (Bi) in high-purity He gas presented a capacity retention of 1500 mA h g^{-1} at 1.8 A g^{-1} after 500 cycles.[19] Recently, we develop an air-oxidation route from Mg_2Si to synthesize nanoporous silicon, which showed 1200 mA h g^{-1} at 1.8 A g^{-1} over 400 cycles.[20]

In this work, we expand the oxidation route of Mg_2Si to synchronously prepare Si@C composites by Mg_2Si powder reacted with ethanol or acetone at 650 °C for 3 h in autoclave, followed by hydrochloric acid washing. The organic solvents such as acetone and ethanol performed not only as oxidizer but also as the source of carbon. The related reaction can be expressed as follows: $Mg_2Si + CH_3COCH_3 \rightarrow Si + C + MgO + C_xH_y$). As lithium ion battery anode, the as-prepared Si@C composites showed a reversible capacity of 3277 mA h g^{-1} at a current density of 0.36 A g^{-1} and remain 892 mA h g^{-1} (85% capacity retention) at 3.6 A g^{-1} over 350 cycles.

2. Results and discussion

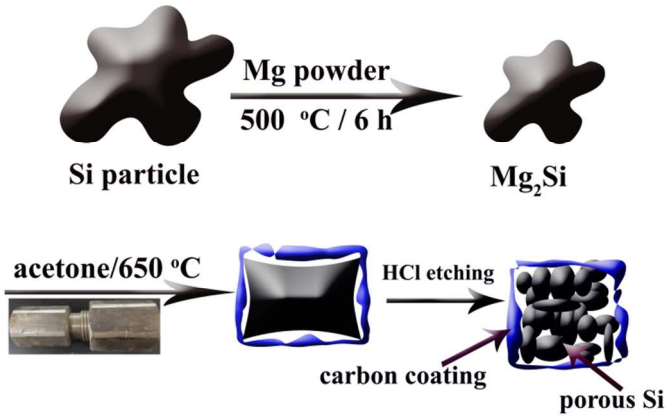

Fig. 1 Schematic illustration of the solvothermal oxidation preparation process of Si@C composites.

Typical fabricating strategy for Si@C composites is schematically illustrated in Fig. 1. The synthesis of Mg_2Si powder has been reported in our previous work.[20] Stoichiometric ratio of acetone and Mg_2Si is sealed in a 20 ml autoclave and heated at 650 °C for 3 h (more details see supplementary information, ESI†). After washed by HCl, the X-ray diffraction (XRD) patterns of the product are shown in Fig. 2a. All the peaks can be indexed to the cubic silicon (JPCDS 27-1402). The Raman spectrum of the as-prepared Si@C composites was displayed in Fig. S1 (ESI†). The peak located at about 520 and 1040 cm^{-1} belongs to the Si. Typical peaks located at approximately 1360 cm^{-1} (D band, disordered) and 1580 cm^{-1} (G band, graphite) are attributed to the carbon. The carbon content was about 20 wt. % according to elemental analysis measurement. Based on the stoichiometric ratio of acetone and Mg_2Si, the content of carbon should be calculated to be about 72 wt. %. The elemental result suggests that only part of carbon from acetone converted into amorphous carbon coating.

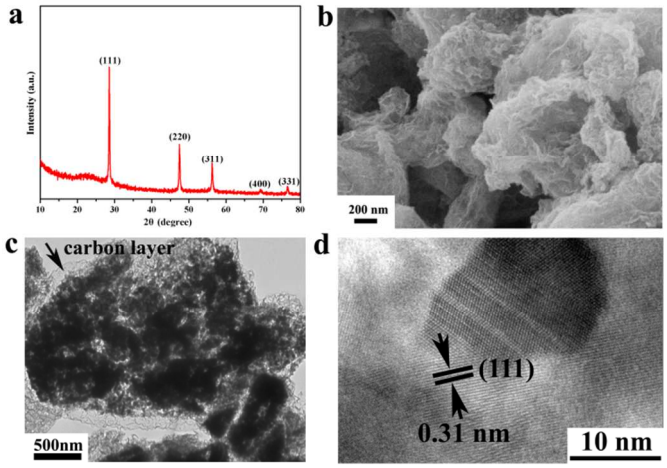

Fig. 2 (a) XRD pattern, (b) SEM image, (c) TEM image and (d) HRTEM image of the as-prepared Si@C composites.

The scanning electron microscopy (SEM) images of the obtained porous Si@C composites are shown in Fig. 2b and Fig. S2 (ESI†). The as-prepared Si@C powder is composed of spherical microparticles with size of 2-5 um. The transmission electron microscopy (TEM) image (Fig. 2c) clearly shows these micropaticles are composed of many nanopartilces and nanopores. What's more, there is a thin layer with thickness about 40 nm coated on the black particles. Fig. 2d is the high-resolution transmission electron microscopy (HRTEM) image of the black particle. The measured interplanar distances is about 0.31 nm belonging to the (111) diffraction peaks of cubic Si. High-angle annular dark-field scanning transmission electron microscopy (HAADF-STEM) and the corresponding EDS mapping images of the as-prepared Si@C composites are displayed in Fig. 3 and Fig. S3 (ESI†). It can be obviously seen

that the carbon is uniformly coated on the Si particle surface. The content of carbon was about 22.21 wt.% (as shown in Fig. S4 ESI†). It is a little higher than the result of elemental analysis, which might result from the less uniformity of the sample. Nitrogen sorption measurements indicate that the Brunauer–Emmett–Teller (BET, Fig. S5a, ESI† for the nitrogen adsorption and desorption isotherms) surface area of the Si@C composites is about 51.2 m^2 g^{-1}. The Barrett–Joyner–Halenda (BJH, Fig. S5b, ESI†) analysis shows that the pore size of the Si@C sample is mainly 4 nm.

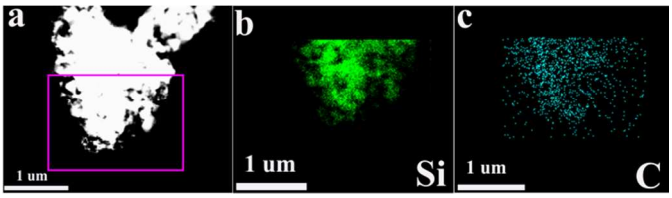

Fig. 3 (a) HAADF-STEM image and the corresponding EDS mapping results of the as-prepared Si@C composites.

In order to investigate the reaction mechanism, experiments with different reaction time are carried out. Fig. 4 shows the XRD patterns of the raw products without acid treatment for different reaction time at 650 °C. After 1 h, the characteristic peaks of cubic Si at 28°, 47.5° and 56.2° which can be indexed to 111, 220 and 311 planes (JCPDS No. 27-1402), can be detected. The peaks of MgO can also be observed. While, there are still some Mg_2Si remained. When the reaction time stretched to 3 h, it is hardly to find the peaks of Mg_2Si in the XRD pattern (Fig. 4c). The diffraction peaks (labelled as ''★'') are characterized as 111, 220, 311, 400, and 331 planes of cubic Si (JCPDS No. 27-1402) and the peaks (labelled as ''•'' JCPDS No. 45-0946) are indexed to 111, 200, 220, 311 and 222 planes of MgO. The related reaction between Mg_2Si and acetone can be expressed as: $Mg_2Si + CH_3COCH_3 \rightarrow Si + C + MgO + C_xH_y$. After washing with HCl, Si@C nanocomposites can be obtained.

Similarly, ethanol can be substituted for acetone to obtain Si@C nanocomposites. The stoichiometric ratio of ethanol and Mg_2Si is sealed in a 20 ml autoclave and heated at 650 °C for 3 h (more details see supplementary information, ESI†). The XRD patterns (as shown in Fig. S6a, ESI†) of the precursor after the solvothermal reaction indicate that the Mg_2Si can also be oxidize by the ethanol, and the raw products detected are MgO and Si. After etched by HCl solution, the crystallization Si material is obtained (as shown in Fig. S6b, ESI†). The Raman spectrum and TEM image (as shown in Fig. S6c and Fig. S6d, ESI†) of the as-prepared materials demonstrated that there is amorphous carbon coated on the surface of the Si particles. Elemental analysis measurement reveals that the carbon content was about 11 wt. %, which is lower than the content of carbon 20% in the Si@C composites obtained using acetone, and is also lower than the 63 wt. % based on the calculation from stoichiometric ratio of ethanol and Mg_2Si.

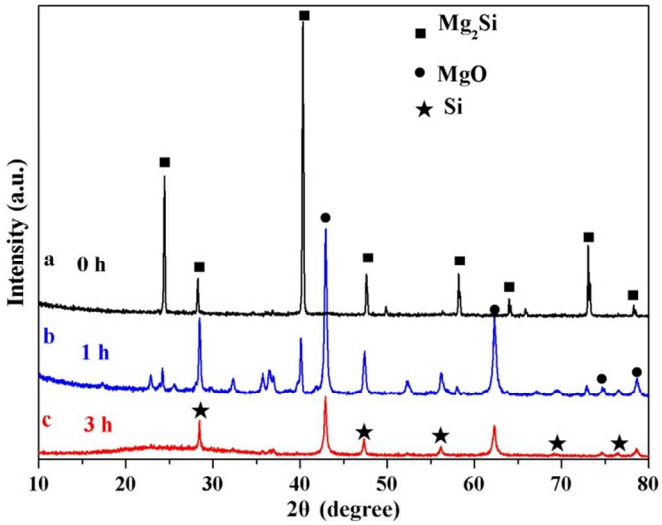

Fig. 4 XRD patterns of precursors at temperature of 650 °C for (a) 0 h, (b) 1 h, (c) 3 h.

The electrochemical properties of the porous Si@C composites anode material were investigated in CR2016 coin cells using lithium foil as a counter electrode. Fig. 5a shows typical voltage curves of Si anode obtained from acetone during the first five cycles in the voltage range of 0.005-1.50 V versus Li/Li^+ at a current density of 0.36 A g^{-1}. In the first cycle, a tiny discharge plateau at about 0.8 V can be assigned to the formation of a solid electrolyte interface (SEI) layer. The plateau at around 0.8 V which disappears in the following cycle results in the initial irreversible capacity loss.[21-23] The discharge plateau located at around 0.2 V belongs to the alloy formation process between Li and crystal Si. Subsequent discharge and charge cycles curves show the voltage profiles characteristic of amorphous Si.[22, 24, 25] The nanoporous Si delivers an initial discharge capacity of 3277 mA h g^{-1} and a charge capacity of 2318 mA h g^{-1}. The initial Coulombic efficiency (CE) is about 71%. After the first cycle, the CE increases to about 99%, suggesting the good reversibility of the nanoporous Si material.

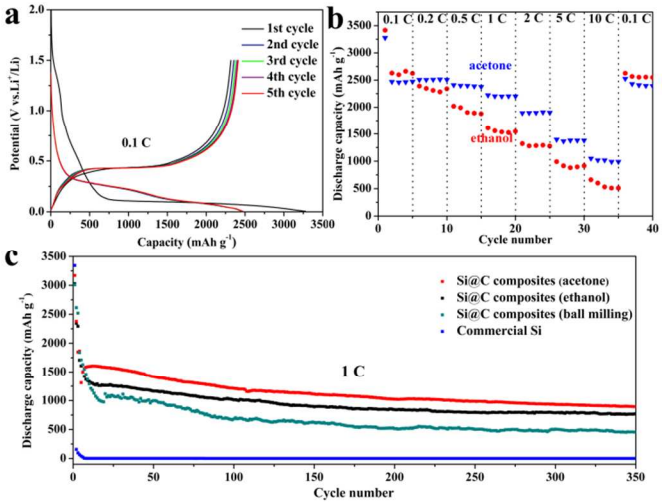

Fig. 5 Electrochemical performances of as-prepared Si@C anode electrodes. (a) First five cycles voltage profiles of acetone reaction obtained at the current density of 0.36 A g^{-1} in the potential region of 0.005-1.50 V versus Li/Li^+. (b) Rate capabilities of the Si@C composites material and (c) long term cycling stability of Si anode at 3.6 A g^{-1} (first five cycle at 0.36 A g^{-1}).

The rate capability for the porous Si anode is shown in Fig. 5b. The measurement current density increases from 0.36 A g^{-1} to 36 A g^{-1} and then goes back to 0.36 A g^{-1}. The Si@C composites obtained from acetone give reversible capacities of about 2500, 2550, 2400, 2200, 1890, 1380 and 1020 mA h g^{-1}. What's more, the CE is almost 100% at different current density. At the high current density of 36 A g^{-1}, the electrode could also exhibit a capacity of 1020 mA h g^{-1} and recover to 2530 mA h g^{-1} as the current density goes back to 0.36 A g^{-1}. Meanwhile, the Si@C composites obtained from ethanol delivers capacity of 2620, 2310, 1990, 1550, 1320, 910 and 530 mA h g^{-1}. The long cycle performance of the porous Si@C composites anode at a current density of 3.6 A g^{-1} is given in Fig. 5c. The cell capacity of commercial Si particles drops very quickly with almost no capacity left after 5 cycles. The Si@C composites prepared by ball milling (more details see Fig. S7, ESI†) exhibit an initial discharge capacity of 3300 mA h g^{-1}, but only remain 500 mA h g^{-1} after 350 cycles. The electrode obtained from the reaction of ethanol delivers the initial discharge capacity of 3027 mA h g^{-1} and remain 770 mA h g^{-1} after 350 cycles. The electrode obtained from the reaction of acetone exhibits an initial capacity of 3190 mA h g^{-1}. X-ray photoelectron spectroscopy (XPS) measurements of the Si@C composites for acetone and ethanol treated materials were carried out (as shown in Fig. S8, ESI†). 2p Si XPS spectras of both Si@C composites for acetone and ethanol treated materials exhibited peak at 103 eV which indicates SiO_2 formation.[26] However, the XPS result of the as-synthesized Si@C composites particles obtained from ethanol showed that the peak intensity at 103 eV is much higher than the peak at 99.8 eV, which indicates that the ethanol treated Si@C composoites have much more silicon oxide than Si@C composoites obtained from acetone on the surface of the porous Si. The much more silicon oxide on the Si particles might result in the lower initial discharge capacity of ethanol treated Si@C composites.[27] After the first five cycles at a current density of 360 mA g^{-1}, the electrode delivers a reversible capacity of 1507 mA h g^{-1}. After 350 discharge/charge cycles, the capacity could still remain 892 mA h g^{-1}. The Si@C composites obtained from acetone exhibit much better rate capability and cyclability than that obtained from ethanol and ball milling.

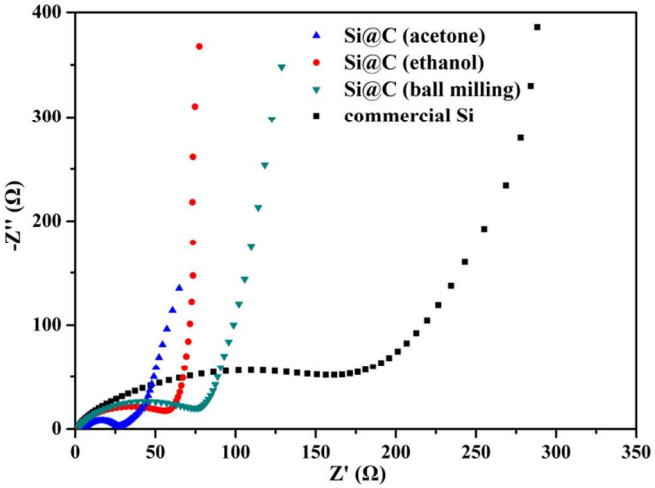

Fig. 6. Nyquist plots for Si@C composites obtained by different methods.

To understand the good electrochemical performance of the Si@C composites obtained from acetone, EIS measurements and TEM were carried out. Nyquist plots (as shown in Fig. 6) displayed that the diameter of the semicircle for Si@C composites obtained from acetone (~ 30 Ω) in the high–medium frequency region was much smaller than that of Si@C composites obtained from ethanol (~ 60 Ω), Si@C composites prepared by ball milling (~ 80 Ω) and commercial Si particles (~ 170 Ω), suggesting that Si@C composites obtained from acetone electrode possesses the highest electronic conductivity among all samples. The morphology and microstructure of the Si@C composites obtained from acetone after 350 cycles were

also carried out using TEM. After 350 cycles, the structure and morphology of the Si@C composites obtained from acetone were similar to its initial state (as shown in Fig. S9, ESI†). However, the shape of the Si@C composites obtained from ethanol was changed and the structure was collapsed. This might result from higher carbon contents of Si@C composites obtained from acetone and much more uniform than that obtained from ethanol. As shown in Fig. 2c and Fig. S6d, the carbon coating of Si@C composites obtained from acetone was much more uniform than that obtained from ethanol. The porous Si particles were entirely and uniformly coated by carbon layer (as shown in Fig. 2c). However, there was some Si particles exposed without carbon coating. After 350 cycles, the carbon coating of Si@C composites obtained from acetone was still coated on the porous Si surface (as shown in Fig. S9, ESI†). As to Si@C composites obtained from ethanol, the carbon coating on the Si particle surface was almost decomposed and could hardly be seen. This might decrease the cyclability and rate capability of the composites obtained from ethanol.[28, 29]

The contribution of the carbon matrix to the performance of the composites was also explored. After etched by HF, the carbon matrix remained its original structure. The initial discharge capacity of the carbon matrix was about 208 mA h g^{-1} (as shown in Fig. 7). After 350 cycles, the capacity remained about 180 mA h g^{-1}. The carbon content of the composite was about 20 wt.%, the contribution of the carbon matrix to the performance of the composite should be about 40 mA h g^{-1}. It was about 1 % of the initial capacity of the composite and 4 % of the total capacity of the composite after 350 cycles, which indicates that the carbon matrix contributes little capacity performance to the composite. The carbon matrix displays important role in improving cycling stability of the composite. To better understand the electrochemical performance during the cycling, TEM analysis was carried out to study the thickness of SEI. As shown in Fig. S10 (ESI†), the SEI layer thickness of the composite was increased as the cycling goes on. After 100 cycles the thickness of the SEI layer was about 200 nm. The SEI thickness was increased to about 400 nm after 350 cycles. When the silicon expands and contracts, the SEI layer deforms and breaks. This might be the main reason that resulted in the capacity decay of the composites.

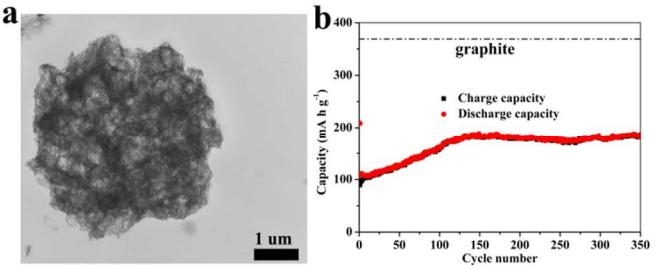

Fig. 7. (a) TEM image of the carbon matrix of the composites after etched by HF, (b) long term cycling properties of the carbon matrix at 0.375 A g^{-1}.

The good electrochemical properties of the samples could be ascribed to both the porous nanostructure and coating of the amorphous carbon layer on the Si particles. The nanostructure gives a short Li^+ diffusion path and electronic transfer distance.[8, 11, 30] Moreover, the void spaces, which generated by removing MgO, leave enough room for expansion and contraction during lithiation and delithiation. The high BET surface of the as-prepared nanoporous Si supply more active sites for the contact between the electrode materials and electrolyte.[21, 29] In-situ carbon coating can enhance the carbon and Si binding force at nanosize and generate homogeneous composites particles.[11, 15] The amorphous carbon layer on the Si nanoparticles can effectively reduces the side reaction with electrolyte and to form stable SEI layers on the Si surface.[27] What's more, the carbon layers increase the electronic conductivity that make sure most Si particles are electrochemically active, which significantly extends the cycle life and improves the rate capability of silicon.[28]

4. Conclusions

In summary, Si@C composites were synchronously synthesized by a solvothermal oxidation reaction of Mg_2Si following by hydrochloric acid washing to remove MgO. The as-prepared Si@C anode material exhibited good stable cycling performance, high rate capability and initial columbic efficiency. Besides acetone, organics such as ethanol could also react with Mg_2Si to form the Si@C composites. This simple solvothermal process might provide a facile way to synchronously synthesize Si@C composites with good lithium storage properties.

Acknowledgements

This work was financially supported by the 973 Project of China (No. 2011CB935901) and the National Natural Science Fund of China (No. 21471142, 21201158).

Notes and references

[a] Hefei National Laboratory for Physical Science at Micro-scale, Department of Chemistry, University of Science and Technology of China, Hefei, Anhui 230026, (P. R. China)
E-mail: ychzhu@ustc.edu.cn; ytqian@ustc.edu.cn
[b] Ningbo Veken Battery Company Inc., West Bonded Zone, Ningbo, Zhejiang 315000, PR China.

† Electronic Supplementary Information (ESI) available: Experimental details, Raman spectrum and SEM image of the as-prepared Si@C composites obtained from the reaction of acetone, nitrogen adsorption curves and pore size distribution of as-prepared silicon obtained from the reaction of acetone, XRD patterns of the precursor and product of the reaction of Mg_2Si with ethanol. Raman spectrum and TEM image of the as-synthesized Si@C composites of the reaction of Mg_2Si with ethanol. XRD pattern, Raman spectrum, SEM image and TEM images of the Si@C composites, which were prepared by ball milling. Nyquist plots for Si@C composites prepared by different methods. TEM images of the Si@C composites after 350 cycles. See DOI: 10.1039/b000000x/

1. M. Obrovac and V. Chevrier, *Chem. Rev.*, 2014, **114**, 11444-11502.
2. U. Kasavajjula, C. Wang and A. J. Appleby, *J. Power Sources*, 2007, **163**, 1003-1039.
3. J. R. Szczech and S. Jin, *Energy Environ. Sci.*, 2011, **4**, 56-72.
4. M. Armand and J.-M. Tarascon, *Nature*, 2008, **451**, 652-657.
5. M. T. McDowell, S. W. Lee, W. D. Nix and Y. Cui, *Adv Mater*, 2013, **25**, 4966-4985.
6. L. Beaulieu, K. Eberman, R. Turner, L. Krause and J. Dahn, *Electrochem. Solid-State Lett.*, 2001, **4**, A137-A140.
7. M. Obrovac and L. Christensen, *Electrochem. Solid-State Lett.*, 2004, **7**, A93-A96.
8. C. K. Chan, H. Peng, G. Liu, K. McIlwrath, X. F. Zhang, R. A. Huggins and Y. Cui, *Nat. Nanotechnol.*, 2008, **3**, 31-35.
9. H. Kim, B. Han, J. Choo and J. Cho, *Angew. Chem.*, 2008, **120**, 10305-10308.
10. A. Magasinski, P. Dixon, B. Hertzberg, A. Kvit, J. Ayala and G. Yushin, *Nat. Mater.*, 2010, **9**, 353-358.
11. H. Wu and Y. Cui, *Nano Today*, 2012, **7**, 414-429.
12. L.-F. Cui, Y. Yang, C.-M. Hsu and Y. Cui, *Nano Lett.*, 2009, **9**, 3370-3374.
13. N. Liu, H. Wu, M. T. McDowell, Y. Yao, C. Wang and Y. Cui, *Nano lett.*, 2012, **12**, 3315-3321.
14. H. Wu, G. Zheng, N. Liu, T. J. Carney, Y. Yang and Y. Cui, *Nano lett.*, 2012, **12**, 904-909.
15. N. Liu, Z. Lu, J. Zhao, M. T. McDowell, H.-W. Lee, W. Zhao and Y. Cui, *Nat. Nanotechnol.*, 2014, **9**, 187-192.
16. X. Li, P. Meduri, X. Chen, W. Qi, M. H. Engelhard, W. Xu, F. Ding, J. Xiao, W. Wang and C. Wang, *J. Mater. Chem.*, 2012, **22**, 11014-11017.
17. W. Li, Y. Tang, W. Kang, Z. Zhang, X. Yang, Y. Zhu, W. Zhang and C. S. Lee, *Small*, 2014, **11**, 1345–1351.
18. L. Wang, N. Lin, J. Zhou, Y. Zhu and Y. Qian, *Chem. Commun.*, 2015, **51**, 2345–2348
19. T. Wada, T. Ichitsubo, K. Yubuta, H. Segawa, H. Yoshida and H. Kato, *Nano Lett*, 2014, **14**, 4505-4510.
20. J. Liang, X. Li, Z. Hou, C. Guo, Y. Zhu and Y. Qian, *Chem. Commun.*, 2015, **51**, 7230-7233.
21. H. Jia, P. Gao, J. Yang, J. Wang, Y. Nuli and Z. Yang, *Adv. Energy Mater.*, 2011, **1**, 1036-1039.
22. J. Maranchi, A. Hepp and P. Kumta, *Electrochem. Solid-State Lett.*, 2003, **6**, A198-A201.
23. Y.-C. Yen, S.-C. Chao, H.-C. Wu and N.-L. Wu, *J. Electrochem. Soc.*, 2009, **156**, A95-A102.
24. J. Li and J. Dahn, *J. Electrochem. Soc.*, 2007, **154**, A156-A161.
25. T. Hatchard and J. Dahn, *J. Electrochem. Soc.*, 2004, **151**, A838-A842.
26. M. R. Alexander, R. Short, F. Jones, W. Michaeli and C. Blomfield, *Appl. Surf. Sci.*, 1999, **137**, 179-183.
27. S. Sim, P. Oh, S. Park and J. Cho, *Adv. Mater.*, 2013, **25**, 4498-4503.
28. J. Saint, M. Morcrette, D. Larcher, L. Laffont, S. Beattie, J. P. Pérès, D. Talaga, M. Couzi and J. M. Tarascon, *Adv. Funct. Mater.*, 2007, **17**, 1765-1774.
29. Z. Lu, N. Liu, H.-W. Lee, J. Zhao, W. Li, Y. Li and Y. Cui, *ACS nano*, 2015, **9**, 2540-2547.
30. M. T. McDowell, S. W. Lee, C. Wang, W. D. Nix and Y. Cui, *Adv. Mater.*, 2012, **24**, 6034-6041.

Table of Content
Synchronously synthesized Si@C composites through solvothermal oxidation of Mg_2Si as lithium ion battery anode

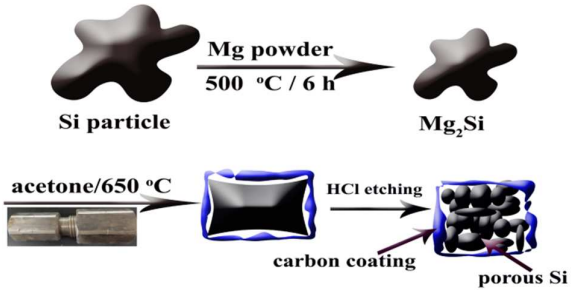

Si@C composites have been synchronously synthesized by solvothermal oxidation of Mg_2Si at 650 °C.